

tively. Stimulating discussions with Professor Weller are gratefully acknowledged.

## References and Notes

- (1) H. Leonhardt and A. Weller, *Ber. Bunsenges. Phys. Chem.*, **67**, 791 (1963).
- (2) N. Mataga, T. Okada, and K. Ezumi, *Mol. Phys.*, **10**, 203 (1966).
- (3) N. Mataga and K. Ezumi, *Bull. Chem. Soc. Jpn.*, **40**, 1355 (1967).
- (4) N. Mataga in "The Exciplex", M. Gordon and W. R. Ware, Ed., Academic Press, New York, 1975, p 144.
- (5) H. Beens and A. Weller in "Organic Molecular Photophysics", Vol. 2, J. B. Birks, Ed., Wiley, New York, 1975, p 201.
- (6) T. Okada, H. Matsui, H. Oohani, H. Matsumoto, and N. Mataga, *J. Chem. Phys.*, **49**, 4717 (1968).
- (7) H. Knibbe, D. Rehm, and A. Weller, *Ber. Bunsenges. Phys. Chem.*, **73**, 839 (1969).
- (8) B. Stevens, *Adv. Photochem.*, **8**, 161 (1971).
- (9) D. Rehm and A. Weller, *Z. Phys. Chem. (Frankfurt am Main)*, **69**, 183 (1970).
- (10) T. R. Evans, *J. Am. Chem. Soc.*, **93**, 2081 (1971).
- (11) (a) D. Rehm and A. Weller, *Ber. Bunsenges. Phys. Chem.*, **73**, 834 (1969); (b) *Isr. J. Chem.*, **8**, 259 (1970); (c) M. T. Indelli and F. Scandola, *J. Am. Chem. Soc.*, **100**, 7734 (1978).
- (12) H. Knibbe, K. Rollig, F. P. Schäfer, and A. Weller, *J. Chem. Phys.*, **47**, 1184 (1967).
- (13) N. Mataga, T. Okada, and N. Yamamoto, *Chem. Phys. Lett.*, **1**, 119 (1967).
- (14) H. Knibbe, D. Rehm, and A. Weller, *Ber. Bunsenges. Phys. Chem.*, **72**, 257 (1968).
- (15) N. Mataga and Y. Mureta, *J. Am. Chem. Soc.*, **91**, 3144 (1969).
- (16) D. V. O'Connor and W. R. Ware, *J. Am. Chem. Soc.*, **101**, 121 (1979).
- (17) W. R. Ware and H. P. Richter, *J. Chem. Phys.*, **48**, 1595 (1968).
- (18) Man-Him and W. R. Ware, *J. Am. Chem. Soc.*, **98**, 4718 (1976).
- (19) (a) M. G. Kuzmin and L. N. Guseva, *Chem. Phys. Lett.*, **3**, 71 (1969); (b) S. P. Van and G. S. Hammond, *J. Am. Chem. Soc.*, **100**, 3895 (1978).
- (20) (a) A. Nakajama, *Bull. Chem. Soc. Jpn.*, **42**, 3409 (1969); (b) N. Nakashima, N. Mataga, F. Ushio, and C. Yamanaka, *Z. Phys. Chem. (Frankfurt am Main)*, **79**, 150 (1972).
- (21) F. Meeus, M. Van der Auweraer, J. C. Dederen, and F. C. De Schryver, *Rec. J. R. Neth. Chem. Soc.*, **98**, 220 (1979).
- (22) M. V. Smoluchowski, *Z. Phys. Chem. (Leipzig)*, **92**, 129 (1917).
- (23) (a) B. J. Berne, "Physical Chemistry, an Advanced Treatise", Vol. VIII, H. Eyring, D. Henderson, and W. Jost, Eds., Academic Press, New York, 1971, p 539; (b) S. W. Benson, "The Foundations of Chemical Kinetics", McGraw-Hill, New York, 1960, p 494.
- (24) (a) R. A. Marcus, *J. Chem. Phys.*, **24**, 966 (1956); *ibid.*, **26**, 867 (1957).
- (25) (a) R. A. Marcus, *J. Chem. Phys.*, **43**, 679 (1965); (b) R. A. Marcus and N. Suttin, *Inorg. Chem.*, **14**, 216 (1975).
- (26) N. Suttin, *J. Photochem.*, **10**, 19 (1979). In this paper  $Z$  is taken equal to  $kT/H$ , whereas the same author in ref 25b takes  $Z$  to be  $10^{11} \text{ M}^{-1} \text{ s}^{-1}$ . In ref 24b Marcus puts  $Z$  equal to  $10^{13} \text{ L mol}^{-1} \text{ s}^{-1}$ ; however, this is changed to  $10^{11} \text{ M}^{-1} \text{ s}^{-1}$  in ref 25a.
- (27) A. Einstein, *Ann. Phys. (Leipzig)*, **17**, 549 (1905).
- (28) Values of  $-2.59$  and  $1 \text{ V}$  are taken for the reduction potential,  $E_{(A/A^-)}$ , of 2MN and the oxidation potential,  $E_{(D/D^+)}$ , of NMP in acetonitrile, according to a reported value of  $E_{(A/A^-)} = -2.57 \text{ V}$  for naphthalene and values for  $E_{(D/D^+)}$  of 0.98 and 1.02 V for TEA and ABCO, respectively.<sup>11</sup>
- (29) R. Ballardini, G. Varani, M. T. Indelli, F. Scandola, and V. Balzani, *J. Am. Chem. Soc.*, **100**, 7219 (1978).
- (30) (a) K. Höfelmann, J. Jagus-Grodzinski, and M. Szwarc, *J. Am. Chem. Soc.*, **91**, 4645 (1979). An Arrhenius activation energy of 2.7 kcal/mol with a preexponential factor equal to  $4 \times 10^{10} \text{ M}^{-1} \text{ s}^{-1}$  is obtained for the rate constant of electron exchange between naphthalenides and naphthalene. If one estimates  $(k_{12}/k_{21}) \omega_{23}$  to be  $10^{11} \text{ M}^{-1} \text{ s}^{-1}$ , then the free energy of activation for this self-exchange electron transfer reaction for naphthalene is 3.2 kcal/mol. (b) N. Hirota, R. Carraway, and W. Shook, *J. Am. Chem. Soc.*, **90**, 3611 (1968).
- (31) A. M. Halpern, *Mol. Photochem.*, **5**, 517 (1973). In the absence of structural interference aliphatic tertiary amines will be nearly planar in the excited state, whereas in the ground state the H-N-H bond angle is  $109^\circ$ .
- (32) M. Kasha and R. Nauman, *J. Chem. Phys.*, **17**, 519 (1949).
- (33) (a) M. Cohen and B. Selinger, *Mol. Photochem.*, **1**, 371 (1969); (b) R. J. McDonald and B. Selinger, *ibid.*, **3**, 101 (1971).
- (34) E. Lippert in ref 5, p 1.
- (35) We neglected the term with  $\delta\epsilon/\delta T$  due to isooctane, which amounts only to  $1.4 \times 10^{-3} \text{ K}^{-1}$ .
- (36) R. A. Marcus, *J. Chem. Phys.*, **43**, 1261 (1965).
- (37) A. M. Halpern, P. Ravinet, and R. J. Sternfels, *J. Am. Chem. Soc.*, **99**, 169 (1977).
- (38) See ref 27, p 553.
- (39) See ref 25a, p 692.
- (40)  $\Delta H^\circ$  is calculated according to  $\Delta H^\circ(\epsilon) = \Delta H^\circ(\text{isooctane}) + \Delta H_b(\epsilon)$ , where  $\mu^2/\rho^3$  was determined to be  $6.300 \text{ cm}^{-1}$  and  $\delta\epsilon/\delta T \approx 1 \times 10^{-2} \text{ K}^{-1}$ .

## Stepwise Bond Dissociation Energies in Sulfur Hexafluoride

T. Kiang and R. N. Zare\*

Contribution from the Department of Chemistry, Stanford University, Stanford, California 94305. Received January 7, 1980

**Abstract:** The  $F_5S-F$  and  $F_3S-F$  bond dissociation energies are determined from studies of the chemiluminescent reactions of  $SF_6$  and  $SF_4$  with metastable calcium and strontium atoms under single-collision conditions. These results are combined with known heats of formation to deduce the following stepwise bond dissociation energies:  $D_0^\circ(F_5S-F) = 91.1 \pm 3.2$ ,  $D_0^\circ(F_4S-F) = 53.1 \pm 6.0$ ,  $D_0^\circ(F_3S-F) = 84.1 \pm 3.0$ ,  $D_0^\circ(F_2S-F) = 63.1 \pm 7.1$ ,  $D_0^\circ(FS-F) = 91.7 \pm 4.3$ ,  $D_0^\circ(S-F) = 81.2 \pm 1.6 \text{ kcal/mol}$ . The zigzag pattern of these successive bond dissociation energies is discussed in terms of bonding theory.

## Introduction

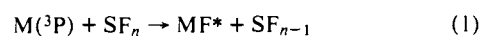
Through advances in high-temperature chemistry, it is now possible to measure the stepwise bond dissociation energies of a number of polyvalent compounds in which a central atom is surrounded by identical ligands.<sup>1</sup> Central atoms belonging to groups 5-8 in the periodic table are of particular interest because these elements have the ability to form more bonds than the Lewis-Langmuir octet rule<sup>2,3</sup> permits. Studies of these "hypervalent"<sup>4</sup> molecules have been greatly stimulated by the discovery of the xenon fluorides.<sup>5</sup>

The sulfur fluorides, particularly the stable gaseous species sulfur tetrafluoride ( $SF_4$ ) and sulfur hexafluoride ( $SF_6$ ), are outstanding examples of hypervalent compounds. The present work reports the determination of the  $F_3S-F$  bond dissociation energy and slightly revises the  $F_5S-F$  bond dissociation energy determined previously in this laboratory.<sup>6</sup> The motivation of

this study is that such measurements can be combined with existing thermochemical and mass spectrometric data to deduce the bond dissociation energies of  $F_{n-1}S-F$ ,  $n = 1-6$ . This structural information can then be used to test various valency concepts in order to deepen our understanding of the bonding in the sulfur fluorides and other hypervalent species.

## Experimental Section

**Method.** Chemiluminescent emission from elementary bimolecular reactions under single-collision conditions provides a means for placing bounds on the bond dissociation energy of the reactant, provided that the bond dissociation energy of the product is known.<sup>6,7</sup> We apply this technique to the reaction of a metastable alkaline earth atom,  $M(^3P)$ , with a sulfur fluoride,  $SF_n$ :



which yields an electronically excited alkaline earth monofluoride,

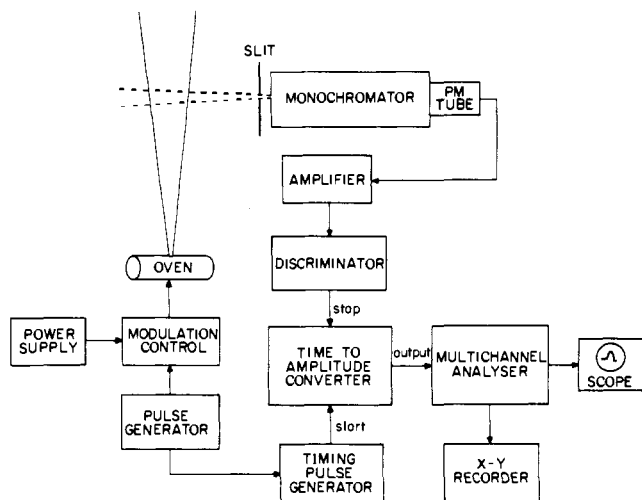


Figure 1. Schematic diagram of the time-of-flight (TOF) chemiluminescence detection system.

MF\*, and the fragment  $SF_{n-1}$ . Detailed energy balance for reaction 1 leads to the equality

$$D_0^\circ(F_{n-1}S-F) + E_{\text{int}}(SF_{n-1}) + E_{\text{trans}}^f = D_0^\circ(M-F) + E_{\text{int}}(M) + E_{\text{int}}(SF_n) - E_{\text{int}}(MF) + E_{\text{trans}}^i \quad (2)$$

for the individual quantum states of the reactants and products, where  $D_0^\circ(F_{n-1}S-F)$  is the (unknown)  $F_{n-1}S-F$  bond dissociation energy,  $D_0^\circ(M-F)$  is the (known)  $M-F$  bond dissociation energy,  $E_{\text{int}}$  is the internal energy measured from the lowest level, and  $E_{\text{trans}}^i$  is the relative translational energy of the reactants (superscript *i*) or the products (superscript *f*).

By resolving the MF\* chemiluminescent spectrum, the highest populated internal state of the product is identified. The assumption is made that in some collisions the maximum reaction exothermicity appears in the MF\* product. Moreover, when MF\* is populated in its highest internal state, the internal energy in the  $SF_{n-1}$  product,  $E_{\text{int}}(SF_{n-1})$ , as well as the final relative translational energy,  $E_{\text{trans}}^f$ , is nearly zero. With the neglect of these latter two quantities, an upper bound is placed on  $D_0^\circ(F_{n-1}S-F)$  from eq 2, since all quantities on the right-hand side of this equation are either known or can be measured directly or estimated.

**Apparatus.** The apparatus used in this study, called LABSTAR, has been described in detail elsewhere.<sup>8,9</sup> A graphite heater tube which houses the metal oven is operated at a temperature corresponding to a metal vapor pressure of 0.1 Torr. A discharge is struck directly by applying a dc voltage across the exit apertures of the oven assembly. A separately pumped vacuum chamber houses the sulfur fluoride source and the reaction zone. The gaseous sulfur fluoride under investigation enters this chamber through a multichannel array and it essentially fills the entire reaction chamber ("beam-gas arrangement").

The chemiluminescence from the reaction zone is observed perpendicular to the metal beam. A 1-m spectrometer (Interactive Technology) views the emission through a quartz port in the reaction chamber. The emission is focused onto the entrance slit and detected at the exit slit by a cooled photomultiplier (Centronic S-20 extended red response). A picoammeter (Keithley Model 417) amplifies the photomultiplier current and drives a strip chart recorder.

To estimate the contribution of reagent translational energy,  $E_{\text{trans}}^i$ , to the internal excitation of the alkaline earth monofluoride, time-of-flight (TOF) spectra are recorded digitally (Figure 1). A narrow slit ( $\sim 2.5$  mm) at the reaction zone defines the viewing region, giving a flight path of 14.0 cm measured from the discharge region to the observation zone. The radiative lifetimes of the excited alkaline earth monohalides are short ( $\sim 20$  ns).<sup>10</sup> Consequently, only chemiluminescence originating from reactive collisions in the observation zone contributes to the TOF signal.

A pulse generator (Hewlett-Packard 8011A) provides synchronization for the TOF measurements. At time  $t = 0$ , a start pulse (positive square shape) of width  $\tau_1$  from the generator triggers the discharge which creates metastable calcium or strontium atoms. The leading edge of the same pulse also starts the ramp voltage in a time-to-

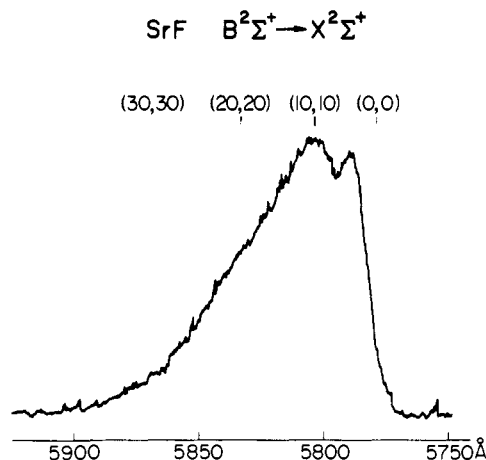


Figure 2. Short-wavelength portion of the Sr(<sup>3</sup>P) + SF<sub>4</sub> chemiluminescent spectrum under single-collision conditions.

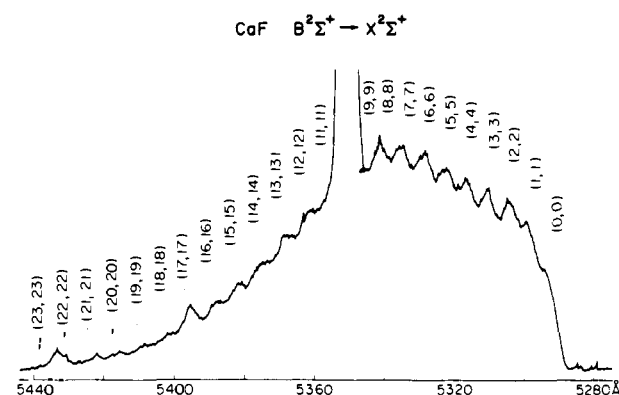


Figure 3. Short-wavelength portion of the Ca(<sup>3</sup>P) + SF<sub>4</sub> chemiluminescent spectrum under single-collision conditions. An atomic line of calcium obscures the (10,10) band.

amplitude converter (TAC; ORTEC Model 467). The current pulses from the photomultiplier tube are amplified, discriminated, and used to stop the ramp voltage in the TAC. The height of the ramp voltage is measured using a pulse height analyzer (Nicolet Model SW-75) and stored in a multichannel analyzer (Nicolet Model 1070). The discharge is turned on and off at a rate of 1 kHz with a pulse duration  $\tau_1 = 50 \mu\text{s}$ . Histograms of 1024 channels are recorded in which the width of each channel is 0.4 or 0.8  $\mu\text{s}$ , depending on whether the TAC is set at a full time range of 400 or 800  $\mu\text{s}$ . For TOF measurements the shorter time range is used for the lighter calcium metastables, since the resulting chemiluminescence occurs at earlier times.

**Reagents.** SF<sub>6</sub> (Matheson, 99.9%) and SF<sub>4</sub> (Matheson, 94%) were both used without further purification. The major contaminant in SF<sub>4</sub> was SOF<sub>2</sub>. In some studies the SF<sub>4</sub> was replaced by SOF<sub>2</sub> (Pfaltz and Bauer,  $\sim 98\%$ ) in order to differentiate between chemiluminescence from reaction with SF<sub>4</sub> and with SOF<sub>2</sub>. Strontium rod (Alfa Products, 99%) and calcium turnings (MCB, 99%) were also used as received.

## Results

**Reactions of Sr(<sup>3</sup>P) and Ca(<sup>3</sup>P) with SF<sub>4</sub>.** Figures 2 and 3 show the short-wavelength portions of the chemiluminescent spectra obtained when metastable strontium and calcium atoms, respectively, react with sulfur tetrafluoride. In both cases the  $B^2\Sigma^+ - X^2\Sigma^+$  band system of the alkaline earth monofluoride is observed, but under the present resolution (5 Å) the SrF B-X system is much less structured than the CaF B-X system. Vibrational assignments are made for the SrF and CaF B-X chemiluminescence based on previous spectroscopic studies.<sup>11,12</sup> Chemiluminescence from the lower electronic states, SrF  $A^2\Pi_{1/2,3/2} - X^2\Sigma^+$  and CaF  $A^2\Pi_{1/2,3/2} - X^2\Sigma^+$  is also observed. Table I lists the highest vibrational level populated,  $v'_{\text{max}}$ , and the corresponding internal energy,  $E_{\text{int}}$ , for

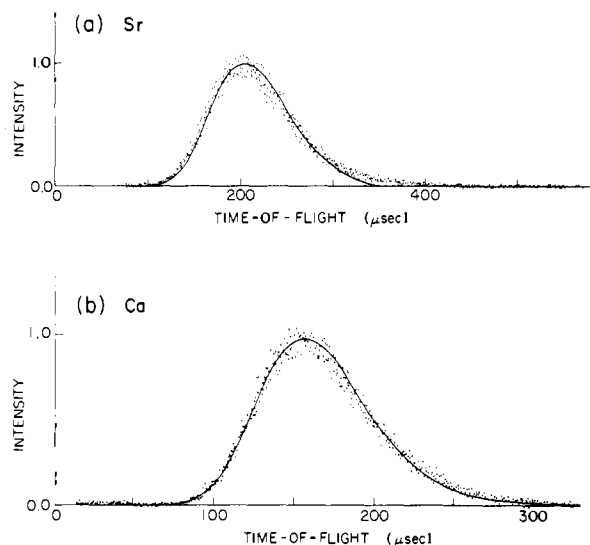


**Figure 4.** Typical time-of-flight spectra: (a) Sr(<sup>3</sup>P) + SF<sub>6</sub>; (b) Ca(<sup>3</sup>P) + SF<sub>6</sub>. The solid curves are the best fit obtained with two adjustable parameters,  $v_0$  and  $\sigma$  (see eq 3 and 4). Both (a) and (b) refer to the entries in Table II for the higher  $v'$  value.

each band system used in calculating the F<sub>3</sub>S–F bond dissociation energy. Similar information is included for the reactions of metastable strontium and calcium atoms with sulfur hexafluoride for comparison purposes.<sup>6</sup> The value of  $v'_{\max}$  is estimated to be no more uncertain than one vibrational quanta.

Thionyl fluoride (SOF<sub>2</sub>), as mentioned previously, is a Sr(<sup>3</sup>P) and Ca(<sup>3</sup>P) also give alkaline earth monofluoride B<sup>2</sup>Σ<sup>+</sup>–X<sup>2</sup>Σ<sup>+</sup> chemiluminescence. Experiments were carried out with pure SOF<sub>2</sub> and compared with those using SF<sub>4</sub>. In the case of Sr(<sup>3</sup>P) + SOF<sub>2</sub> the highest vibrational level populated is about four quanta lower than in Sr(<sup>3</sup>P) + SF<sub>4</sub>, and in Ca(<sup>3</sup>P) + SOF<sub>2</sub> one quanta lower than in Ca(<sup>3</sup>P) + SF<sub>4</sub>. Consequently, in both cases the presence of trace amounts of SOF<sub>2</sub> in SF<sub>4</sub> does not affect the calculation of the F<sub>3</sub>S–F bond dissociation energy based on the values of  $E_{\text{int}}$  in Table I.

**Time-of-Flight (TOF) Data.** With the value of  $E_{\text{int}}$  (MF) secured from an analysis of the single-collision chemiluminescence spectrum, knowledge is next needed of the role played by reagent relative translational energy,  $E^i_{\text{trans}}$ , in populating the highest vibrational level,  $v'_{\max}$ , observed in the MF\* product. This information is obtained by investigating the time delay between the start of the pulsed discharge making metastables and the first appearance of chemiluminescent features at a fixed wavelength.

Figure 4 presents two typical chemiluminescence TOF spectra, one for reaction of SF<sub>6</sub> with Sr(<sup>3</sup>P) (Figure 4a), the other for reaction of SF<sub>6</sub> with Ca(<sup>3</sup>P) (Figure 4b). In both cases the spectrometer isolates part of the  $\Delta v = 0$  sequence of the B<sup>2</sup>Σ<sup>+</sup>–X<sup>2</sup>Σ<sup>+</sup> system with a resolution of 20–30 Å. Because this resolution is insufficient to observe single vibrational bands, these spectra represent the composite signal from a cluster of neighboring bands. Table II summarizes the range of vibrational levels covered in each study. Note that the TOF spectra show the expected behavior in that the lighter Ca atom produces chemiluminescence at an earlier time than the heavier Sr atom.

The theory of the single-disk TOF method is well known.<sup>9,13</sup> TOF signals are derived from an assumed Gaussian particle flux density

$$I(v) = Nv^3 \exp[-(v - v_0)^2/\sigma^2] \quad (3)$$

where  $N$  is a normalization constant and  $v_0$  and  $\sigma$  are adjustable parameters. Using previously defined experimental ob-

**Table I.** Chemiluminescent Energetics

reaction	electronic state	$v'_{\max}$	$E_{\text{int}}$ (MF), kcal/mol
Sr( <sup>3</sup> P) + SF <sub>4</sub>	SrF B <sup>2</sup> Σ <sup>+</sup>	35 ± 1	91.3 ± 1.0
	A <sup>2</sup> Π <sub>3/2</sub>	≤ 39 ± 1	< 91.2 ± 1.0
	A <sup>2</sup> Π <sub>1/2</sub>	≤ 40 ± 1	< 91.3 ± 1.0
Sr( <sup>3</sup> P) + SF <sub>6</sub>	SrF C <sup>2</sup> Π <sub>1/2,3/2</sub>	5 ± 1	85.1 ± 1.2
	B <sup>2</sup> Σ <sup>+</sup>	24 ± 1	80.2 ± 1.2
	A <sup>2</sup> Π <sub>3/2</sub>	~ 26 ± 1	~ 77.8 ± 1.0
	A <sup>2</sup> Π <sub>1/2</sub>	~ 27 ± 1	~ 78.1 ± 1.0
Ca( <sup>3</sup> P) + SF <sub>4</sub>	CaF B <sup>2</sup> Σ <sup>+</sup>	22 ± 1	83.4 ± 1.1
Ca( <sup>3</sup> P) + SF <sub>6</sub>	CaF B <sup>2</sup> Σ <sup>+</sup>	14 ± 1	75.7 ± 1.4

**Table II.** TOF Analysis of the Chemiluminescent Spectrum

reaction	$v'^a$	$v_0$ , 10 <sup>4</sup> cm/s	$\sigma$ , 10 <sup>4</sup> cm/s	$\bar{E}^i_{\text{trans}}$ , kcal/mol
Sr( <sup>3</sup> P) + SF <sub>4</sub>	22 ± 3	0.80	4.57	2.60
	8 ± 3	2.50	3.89	2.81
Sr( <sup>3</sup> P) + SF <sub>6</sub>	3 ± 2	2.50	3.83	3.03
	2 ± 2	2.60	3.83	3.04
Ca( <sup>3</sup> P) + SF <sub>4</sub>	13 ± 2	3.20	5.76	3.14
	7 ± 2	3.30	5.76	3.18
Ca( <sup>3</sup> P) + SF <sub>6</sub>	7 ± 2	3.50	5.39	3.18
	3 ± 2	3.00	5.39	2.97

<sup>a</sup> The value of  $v'$  refers to the vibrational level at the center of the  $\Delta v = 0$  cluster isolated by the spectrometer.

servables, namely, the flight path  $L$ , the rectangular gate function or beam "on" time  $\tau_1$ , and the observation time  $\tau_2$ , the TOF signal  $F$ , as a function of the flight time,  $T$ , is given by

$$F(T) = \int_0^{\tau_1} dt \int_{v_1(t)}^{v_2(t)} I(v) dv \quad (4)$$

where the limits of the second integral are

$$v_1(t) = L/(T + \tau_2 - t) \quad (5)$$

and

$$v_2(t) = L/(T - t) \quad (6)$$

The parameters  $v_0$  and  $\sigma$  are determined by fitting the observed TOF spectra to computer simulations. This fitting procedure is not a least-squares analysis; instead,  $v_0$  and  $\sigma$  are found by matching the signal peak and the signal half-widths. The values obtained are also displayed in Table II.

No correction is made for the decay of the metastable atoms during the flight time. While the radiative lifetime of the Ca(<sup>3</sup>P<sub>1</sub>) or the Sr(<sup>3</sup>P<sub>1</sub>) fine structure levels is shorter than the flight time,<sup>14</sup> this is not true for the higher lying Ca(<sup>3</sup>P<sub>2</sub>) or Sr(<sup>3</sup>P<sub>2</sub>) levels, whose reactions are assumed to populate the highest vibrational levels observed in MF\*.

Figure 5 illustrates the resulting translational energy distribution of the collision partners in the center-of-mass frame, assuming that the molecular beam flux is described by eq 3. Average translational energies,  $\bar{E}^i_{\text{trans}}$ , are also calculated, and their values are listed in Table II. Although the translational-energy distributions in Figure 5 are broad, the influence of reagent relative translational energy on product vibration is quite small since the values of  $\bar{E}^i_{\text{trans}}$  deduced for different clusters of vibrational levels differ only slightly from one another. Thus, these measurements exclude the possibility that the reagents in the high-energy tail of the Boltzmann distribution cause the population of the highest internal state,  $v'_{\max}$ , of the product. Hence, the value of  $\bar{E}^i_{\text{trans}}$  for the highest vibrational cluster studied is equated to  $E^i_{\text{trans}}$  in calculating bond dissociation energies.

**Bond Dissociation Energies.** By neglecting the terms  $E^f_{\text{trans}}$  and  $E_{\text{int}}(\text{SF}_{n-1})$  in eq 2, upper bounds on the F<sub>3</sub>S–F and

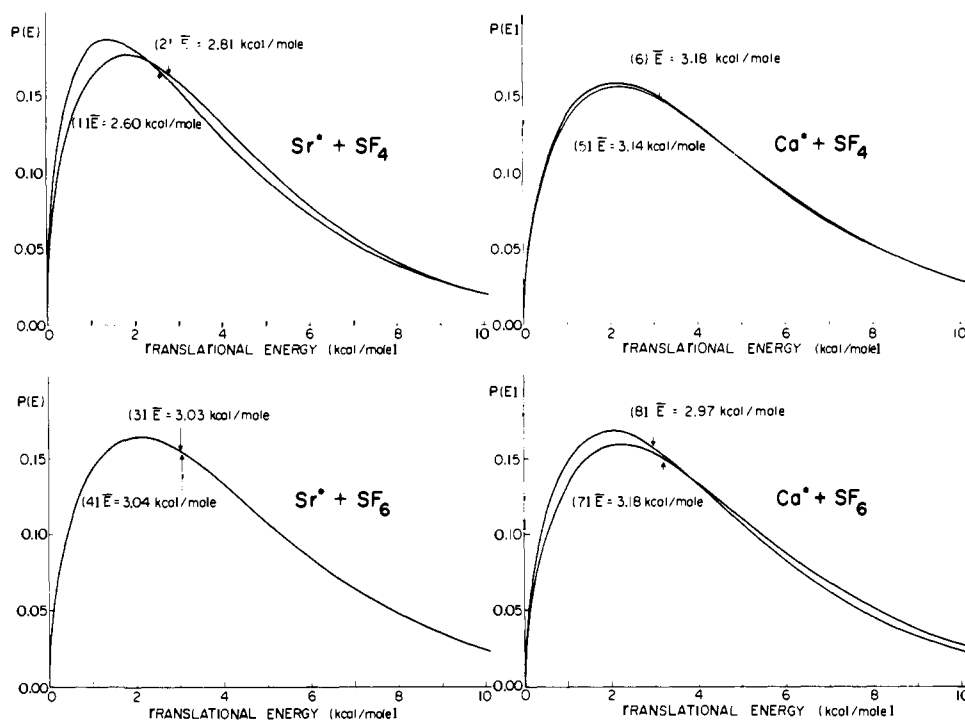


Figure 5. Reagent relative translational energy distributions derived from the time-of-flight parameters listed in Table II. The average energy,  $\bar{E}_{\text{trans}}$ , is marked for each distribution.

$F_5S-F$  bond dissociation energies may be derived for each reaction with metastable Sr or Ca. This inequality uses the values of  $E_{\text{int}}(\text{MF})$  given in Table I,  $E_{\text{trans}}^1 = \bar{E}_{\text{trans}}$  in Table II,  $E_{\text{int}}[\text{Sr}(^3P_2)] = 42.6$  kcal/mol, and  $E_{\text{int}}[\text{Ca}(^3P_2)] = 43.8$  kcal/mol, the average internal energy of  $\text{SF}_4$  (2.2 kcal/mol) and  $\text{SF}_6$  (2.6 kcal/mol) at 298 K, and the known<sup>15</sup> alkaline earth monofluoride bond dissociation energies,  $D_0^\circ(\text{SrF}) = 128.0 \pm 2.0$  and  $D_0^\circ(\text{CaF}) = 127.1 \pm 2.0$  kcal/mol. The results are

$$\begin{aligned} D_0^\circ(\text{F}_3\text{S}-\text{F}) &\leq 84.1 \pm 3.0 \text{ kcal/mol} & \text{SF}_4 + \text{Sr}(^3\text{P}) \\ D_0^\circ(\text{F}_3\text{S}-\text{F}) &\leq 89.9 \pm 3.3 \text{ kcal/mol} & \text{SF}_4 + \text{Ca}(^3\text{P}) \\ D_0^\circ(\text{F}_5\text{S}-\text{F}) &\leq 91.1 \pm 3.2 \text{ kcal/mol} & \text{SF}_6 + \text{Sr}(^3\text{P}) \\ D_0^\circ(\text{F}_5\text{S}-\text{F}) &\leq 101.0 \pm 3.4 \text{ kcal/mol} & \text{SF}_6 + \text{Ca}(^3\text{P}) \end{aligned}$$

Interestingly, the strontium metastable reactions give the smaller upper bound, although, in the case of reactions with thionyl fluoride, the calcium and strontium metastables lead to the same value of the dissociation energy [ $D_0^\circ(\text{FOS}-\text{F}) = 86.5 \pm 4.0$  kcal/mol].<sup>16</sup> It is not clear presently why the reactions of  $\text{SF}_4$  and  $\text{SF}_6$  with  $\text{Ca}(^3\text{P})$  do not lead to the appearance of all the reaction exothermicity in the  $\text{CaF}$  product for some reactive encounters. However, in the absence of information to the contrary, the upper bounds determined from the reactions of  $\text{SF}_4$  and  $\text{SF}_6$  with  $\text{Sr}(^3\text{P})$  are believed to represent the actual dissociation energies within the stated uncertainties.

The value for the  $\text{F}_3\text{S}-\text{F}$  bond dissociation energy,  $84.1 \pm 3.0$  kcal/mol, found in this study is in close agreement with the previous value of  $83.9 \pm 1.2$  kcal/mol determined by Harland and Thynne<sup>17</sup> in their dissociative electron attachment experiment but is somewhat larger than the value of 79.0 kcal/mol used by Bott<sup>18</sup> in correlating his shock tube dissociation data of  $\text{SF}_4$  with RRK theory. The value for the  $\text{F}_5\text{S}-\text{F}$  bond dissociation energy,  $91.1 \pm 3.2$  kcal/mol, is slightly revised from the previous value of  $89.9 \pm 3.4$  kcal/mol found by the same method.<sup>6</sup> The change arises from the improved estimate of  $E_{\text{trans}}^1$  based on time-of-flight measurements of the chemi-

Table III. Heats of Formation of the Sulfur Fluorides, Sulfur, and Fluorine

species (gas)	$\Delta H_{\text{f}0}^\circ$ , kcal/mol	ref
S	$65.7 \pm 0.1$	20a
F	$18.4 \pm 0.4$	20a
SF	$2.9 \pm 1.5$	20b
SF <sub>2</sub>	$-70.4 \pm 4.0$	20b
SF <sub>3</sub>	$-115.2 \pm 5.8$	present work <sup>a</sup>
SF <sub>4</sub>	$-180.9 \pm 5.0$	20b
SF <sub>5</sub>	$-215.7 \pm 3.2$	present work <sup>b</sup>
SF <sub>6</sub>	$-288.4 \pm 0.2$	20b

<sup>a</sup> In ref 20b the value of  $\Delta H_{\text{f}0}^\circ(\text{SF}_3)$  is given as  $-119.3 \pm 8.0$  kcal/mol, based on the average of previous  $\text{F}_3\text{S}-\text{F}$  bond dissociation energies. <sup>b</sup> In ref 20b the value of  $\Delta H_{\text{f}0}^\circ(\text{SF}_5)$  is given as  $-231.7 \pm 5$  kcal/mol, based on a previous (incorrect)  $\text{F}_5\text{S}-\text{F}$  bond dissociation energy.

luminescent spectrum. The comparison with other literature values has been discussed previously.<sup>6,19</sup>

Based on previous thermochemical and mass spectrometric studies,<sup>20,21</sup> the heats of formation,  $\Delta H_{\text{f}0}^\circ$ , of F, S, SF, SF<sub>2</sub>, SF<sub>4</sub>, and SF<sub>6</sub> are known, and the values are summarized in Table III. The new bond dissociation energies for SF<sub>4</sub> and SF<sub>6</sub> found in this study permit the evaluation of the other heats of formation from the relations

$$\Delta H_{\text{f}0}^\circ(\text{SF}_5) = D_0^\circ(\text{F}_5\text{S}-\text{F}) + \Delta H_{\text{f}0}^\circ(\text{SF}_6) - \Delta H_{\text{f}0}^\circ(\text{F}) \quad (7)$$

and

$$\Delta H_{\text{f}0}^\circ(\text{SF}_3) = D_0^\circ(\text{F}_3\text{S}-\text{F}) + \Delta H_{\text{f}0}^\circ(\text{SF}_4) - \Delta H_{\text{f}0}^\circ(\text{F}) \quad (8)$$

These results are also listed in Table III. Once the heats of formation of all sulfur fluorides are known, then the bond dissociation energies may be determined from the relation

$$D_0^\circ(\text{F}_{n-1}\text{S}-\text{F}) = \Delta H_{\text{f}0}^\circ(\text{SF}_{n-1}) + \Delta H_{\text{f}0}^\circ(\text{F}) - \Delta H_{\text{f}0}^\circ(\text{SF}_n) \quad (9)$$

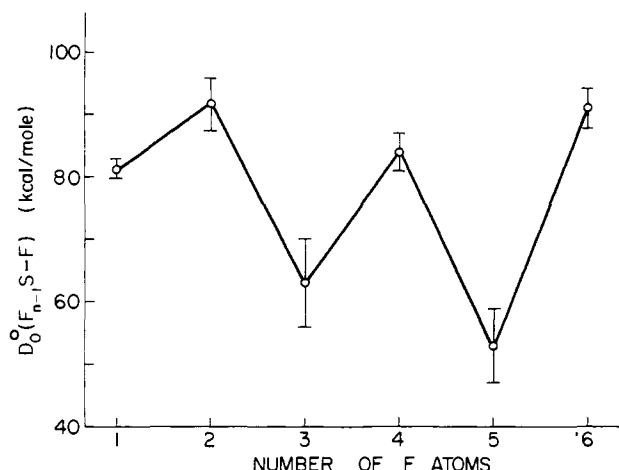


Figure 6. The sulfur fluoride bond dissociation energies as a function of the number of fluorine atoms.

Table IV displays the stepwise bond dissociation energies where the uncertainty is calculated from the propagation of errors using the uncertainties in the individual quantities.

### Discussion

A plot of the stepwise bond dissociation energies  $D_0^\circ(F_{n-1}S-F)$  of  $SF_6$  as a function of  $n$ , the number of fluorine atoms, is shown in Figure 6. A systematic pattern is at once apparent; successive bond dissociation energies alternate in magnitude, the even members being larger than the odd ones. This zigzag pattern for  $SF_6$  has been noted previously by Hildenbrand,<sup>21</sup> who suggested that its origin could be rationalized in terms of hybridization concepts<sup>3,22</sup> for bonding.

According to this valence-bond picture, the sulfur atom with its  $3s^23p^4$  configuration can form two p bonds directly without valence excitation. It may be thought that these bonds are not pure p in character but involve some s participation in the form of s-p hybridization. This valence excitation occurs with the formation of the first S-F bond, thereby reducing its bond dissociation energy. The formation of  $FSF$  from F and SF needs no additional valence excitation so that  $D_0^\circ(S-F) < D_0^\circ(FS-F)$ , as is observed. To form  $SF_3$  and  $SF_4$ , it is necessary in this model to promote one of the electrons in an s orbital to a d orbital yielding  $sp^3d$  hybrids, which have the geometrical shape of an irregular tetrahedron. This electron rearrangement comes at the expense of the first new bond, causing  $D_0^\circ(F_2S-F) < D_0^\circ(F_3S-F)$ . A further promotion of an electron to a d orbital is required upon addition of the fifth fluorine as the  $sp^3d^2$  hybridization having octahedral symmetry is achieved. Again this has the energetic implication that  $D_0^\circ(F_4S-F) < D_0^\circ(F_5S-F)$ . In this manner the valence-bond picture provides a qualitative explanation for the observed zigzag pattern of the  $SF_6$  stepwise bond dissociation energies.

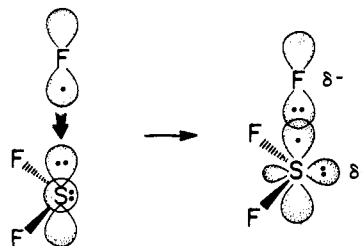
An essential aspect of this description for the bonding in the hypervalent sulfur fluorides,  $SF_3$ ,  $SF_4$ ,  $SF_5$ , and  $SF_6$ , is the concept of an expanded valence shell whereby the central sulfur atom uses d orbitals to form additional bonds. However, the promotion energies of atomic d orbitals on sulfur are so large ( $>190$  kcal/mol) that this casts doubt upon this model. Indeed, recent semiempirical<sup>23</sup> as well as ab initio<sup>24</sup> calculations on the electronic structure of the sulfur fluorides show that d-orbital participation is minor and need not be invoked to explain either the bonding strength or the geometry of  $SF_4$  and  $SF_6$ .

An alternative view, first introduced by Pimentel<sup>25</sup> and by Rundle<sup>26</sup> to explain the bonding of the polyhalide ions and later elaborated on by others,<sup>4,23,24,27</sup> is that the bonding involves delocalized combinations of atomic orbitals which are mainly

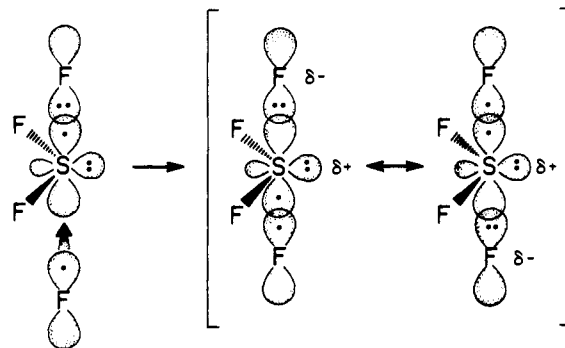
Table IV. Primary Bond Dissociation Energies of the Sulfur Fluorides

species	$D_0^\circ$ , kcal/mol	species	$D_0^\circ$ , kcal/mol
SF	$81.2 \pm 1.6$	$SF_4$	$84.1 \pm 3.0$
$SF_2$	$91.7 \pm 4.3$	$SF_5$	$53.1 \pm 6.0$
$SF_3$	$63.1 \pm 7.1$	$SF_6$	$91.1 \pm 3.2$

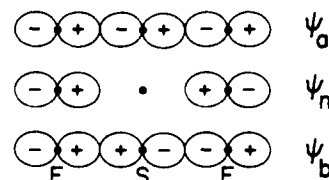
p orbitals. In this model an F atom approaches one of the lone pairs on  $SF_2$  and forms a weak two-center three-electron bond which is ionic in character; i.e., one electron of the lone pair on S fills the hole on F to give the more electronegative ligand a closed shell  $F^-SF_2^+$  structure:



The next fluorine atom approaches from the opposite direction, forming a strong three-center four-electron bond:



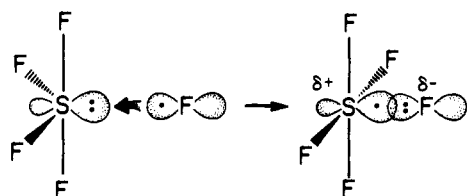
This type of bonding requires that the terminal atoms be more electronegative than the central atom. From a molecular-orbital viewpoint, there are three orbitals associated with the axial F-S-F bonds in  $SF_4$ :



One molecular orbital,  $\psi_b$ , is the in-phase overlap of the p orbitals on F with the p orbital on S directed along the F-S-F axis. It is bonding but withdraws electron density from S, giving ionic as well as covalent character. Another molecular orbital,  $\psi_n$ , represents p orbitals on the terminal atoms, alone, and its character is nonbonding. The third molecular orbital,  $\psi_a$ , is the out-of-phase overlap of the p orbitals on F with the p orbital on S and it is antibonding in character. In the axial F-S-F part of  $SF_4$ , four valence electrons are available, two occupying the bonding three-center orbital,  $\psi_b$ , and two occupying the nonbonding orbital,  $\psi_n$ . Consequently, one expects that the axial F atoms have a longer bond length<sup>28</sup> and a lower dissociation energy than the equatorial F atoms. This model is also consistent with the fact that electronegative substituents prefer the axial sites of sulfuranes.<sup>23h,29</sup>

This story essentially repeats itself in constructing  $SF_5$  and  $SF_6$ .  $SF_5$  is built up from  $SF_4$  and F by having the F atom approach the last lone pair on  $SF_4$  to form a weak two-center

three-electron F<sup>-</sup>-SF<sub>4</sub><sup>+</sup> bond. At the same time, an electron rearrangement occurs in the SF<sub>4</sub><sup>+</sup> part of the molecule so that there are two three-center four-electron bonds, giving SF<sub>5</sub> the structure of a tetragonal pyramid.<sup>30</sup>



SF<sub>6</sub> is built up from SF<sub>5</sub> and F by the formation of a strong three-center four-electron bond when F approaches SF<sub>5</sub> from the opposite side of the F<sup>-</sup>-SF<sub>4</sub><sup>+</sup> bond. In SF<sub>6</sub> the maximum number of ligands is reached and by symmetry all S-F bonds are equivalent; i.e., SF<sub>6</sub> has three orthogonal three-center four-electron bonds.

Thus this transformation of lone-pair electrons on the central sulfur atom to at first a weak two-center three-electron bond and then to a strong three-center four-electron bond permits sulfur to have a hypervalent character without introducing the concepts of valence excitation and d-orbital hybridization. Moreover, this simple picture also accounts for the observed alternation of the stepwise bond dissociation energies in going from SF<sub>6</sub> to SF<sub>2</sub>. It may be expected that similar behavior will be found in the successive bond dissociation energies of other hypervalent compounds.

**Acknowledgments.** We thank D. L. Hildenbrand, R. H. Holm, and W. R. Wadt for useful discussions. This work was supported by the Army Research Office under DAAG 29-77-G-0151.

## References and Notes

- Hildenbrand, D. L. *Adv. High Temp. Chem.* **1967**, *1*, 193.
- (a) Lewis, G. N. *J. Am. Chem. Soc.* **1916**, *38*, 762. (b) Langmuir, I. *ibid.* **1919**, *41*, 868, 1543.
- (a) Pauling, L. "The Nature of the Chemical Bond", 3rd ed.; Cornell University Press: Ithaca, N.Y., 1960. (b) *J. Am. Chem. Soc.* **1931**, *53*, 1367.
- Musher, J. I. *Angew. Chem., Int. Ed. Engl.* **1969**, *8*, 54.
- (a) Chernick, C. L.; Claassen, H. H.; Fields, P. R.; Hyman, H. H.; Malm, J. G.; Manning, W. M.; Matheson, M. S.; Quaterman, L. A.; Schreiner, F.; Selig, H. H.; Sheft, I.; Siegel, S.; Sloth, E. N.; Stein, L.; Studier, M. H.; Weeks, J. L.; Zirin, M. H. *Science* **1962**, *138*, 136. (b) Claassen, H. H.; Selig, H.; Malm, J. G. *J. Am. Chem. Soc.* **1962**, *84*, 3593. (c) Weeks, J. L.; Chernick, C. L.; Matheson, M. S. *ibid.* **1962**, *84*, 4612.
- Kiang, T.; Estler, R. C.; Zare, R. N. *J. Chem. Phys.* **1979**, *70*, 5925.
- Zare, R. N. *Ber. Bunsenges. Phys. Chem.* **1974**, *78*, 153.
- Oldenborg, R. C.; Dickson, C. R.; Zare, R. N. *J. Mol. Spectrosc.* **1975**, *58*, 283.
- Estler, R. C.; Zare, R. N. *Chem. Phys.* **1978**, *28*, 253.
- Dagdigian, P. J.; Cruse, H. W.; Zare, R. N. *J. Chem. Phys.* **1974**, *60*, 2330.
- Menzinger, M. *Can. J. Chem.* **1974**, *52*, 1688.
- Steimle, T. C.; Domaille, P. J.; Harris, D. O. *J. Mol. Spectrosc.* **1977**, *68*, 134.
- Gally, T. D.; Rosner, S. D.; Holt, R. A. *Rev. Sci. Instrum.* **1976**, *47*, 143.
- (a) Havey, M. D.; Balling, L. C.; Wright, J. J. *Phys. Rev. A* **1976**, *13*, 1269. (b) Giustfredi, G.; Minguzzi, P.; Strumia, F.; Tonelli, M. Z. *Phys. A* **1975**, *274*, 279. (c) Furcinitti, P. S.; Balling, L. C.; Wright, J. J. *Phys. Lett. A* **1975**, *53*, 75.
- See: Karny, Z.; Zare, R. N. *J. Chem. Phys.* **1978**, *68*, 3360. These bond energies agree within the stated uncertainties with the values reported in Hildenbrand, D. L. *ibid.* **1968**, *48*, 3647.
- Kiang, T.; Zare, R. N., in preparation.
- Harland, P. W.; Thynne, J. C. J. *J. Phys. Chem.* **1971**, *75*, 3517.
- Bott, J. F. *J. Chem. Phys.* **1971**, *54*, 181.
- Since ref 6 was completed, B. S. Rabinovitch (private communication) has pointed out to us that the calculation of D<sub>0</sub><sup>0</sup>(F<sub>5</sub>-S-F) from the shock tube dissociation data (Bott, J. F.; Jacobs, T. A. *J. Chem. Phys.* **1969**, *50*, 3850. Lyman, J. L. *ibid.* **1977**, *67*, 1868. Benson, S. W. *Chem. Rev.* **1978**, *78*, 23) may be an overestimate since no variation of the collision efficiency with the degree of falloff was considered. See: Rabinovitch, B. S.; Keil, D. G.; Burkhalter, J. F.; Skinner, G. B. Proceedings of the Tenth International Shock Tube Symposium, Kyoto, Japan, 1975.
- (a) Stull, D. R., Ed. "JANAF Thermochemical Tables"; Dow Chemical Co.: Midland, Mich., 1965. (b) Chase et al. *J. Phys. Chem. Ref. Data*, **1978**, *7*, 897-917.
- Hildenbrand, D. L. *J. Phys. Chem.* **1973**, *77*, 897.
- (a) Skinner, H. A. *Trans. Faraday Soc.* **1949**, *45*, 20. (b) *ibid.* **1955**, *51*, 1036.
- (a) Willett, R. D. *Theor. Chim. Acta* **1964**, *2*, 393. (b) Santry, D. P.; Segal, G. A. *J. Chem. Phys.* **1967**, *47*, 158. (c) Santry, D. P. *J. Am. Chem. Soc.* **1968**, *90*, 3309. (d) Brown, R. D.; Peel, J. B. *Aust. J. Chem.* **1968**, *21*, 2589, 2605, 2617. (e) Gavin, R. M. Jr. *J. Chem. Educ.* **1969**, *46*, 413. (f) Companion, A. L. *Theor. Chim. Acta* **1972**, *25*, 268. (g) Koutecký, V. B.; Musher, J. I. *ibid.* **1974**, *33*, 227. (h) Chen, M. M. L.; Hoffmann, R. *J. Am. Chem. Soc.* **1976**, *98*, 1647. (i) Rösch, N.; Smith, V. H.; Whangbo, M. H. *Inorg. Chem.* **1976**, *15*, 1768. (j) Cowley, A. H.; Lattman, M.; Walker, M. L. *J. Am. Chem. Soc.* **1979**, *101*, 4074.
- (a) Radom, L.; Schaefer, H. F. III. *Aust. J. Chem.* **1975**, *28*, 2069. (b) Hay, P. J. *J. Am. Chem. Soc.* **1977**, *99*, 1003, 1013.
- Pimentel, G. C. *J. Chem. Phys.* **1951**, *19*, 446.
- (a) Hach, R. J.; Rundle, R. E. *J. Am. Chem. Soc.* **1951**, *73*, 4321. (b) Rundle, R. E. *Rec. Chem. Prog.* **1962**, *23*, 195. (c) *J. Am. Chem. Soc.* **1963**, *85*, 112. (d) *Surv. Prog. Chem.* **1963**, *1*, 81.
- (a) Cornwell, C. D.; Yamasaki, R. S. *J. Chem. Phys.* **1957**, *27*, 1060. (b) Yamasaki, R. S.; Cornwell, C. D. *ibid.* **1959**, *30*, 1265. (c) Wiebenga, E. H.; Havinga, E. E.; Boswijk, K. H. *Adv. Inorg. Chem. Radiochem.* **1961**, *3*, 133. (d) Bersohn, R. *J. Chem. Phys.* **1962**, *36*, 3445. (e) Jortner, J.; Rice, S. A.; Wilson, E. G. *ibid.* **1963**, *38*, 2302. (f) Bersohn, R. *ibid.* **1963**, *38*, 2913. (g) Pitzer, K. S. *Science* **1963**, *139*, 414. (h) Malm, J. G.; Selig, H.; Jortner, J.; Rice, S. A. *Chem. Rev.* **1965**, *65*, 199. (i) Coulson, C. A. *J. Chem. Phys.* **1968**, *44*, 468.
- Tolles, W. M.; Gwinn, W. D. *J. Chem. Phys.* **1962**, *36*, 1119.
- Muetterties, E. L.; Schunn, R. A. *Q. Rev., Chem. Soc.* **1966**, *20*, 245.
- Gregory, A. R. *Chem. Phys. Lett.* **1974**, *28*, 552.

## Covalent Attachment of Arenes to SnO<sub>2</sub>-Semiconductor Electrodes

Marye Anne Fox,\* Frédéric J. Nobs, and Tamara A. Voynick

Contribution from the Department of Chemistry, University of Texas at Austin, Austin, Texas 78712. Received August 14, 1979

**Abstract:** The synthesis and chemical and physical properties of some arene-derivatized tin oxide semiconductor electrodes are described. Several techniques for attachment are employed (esterification, silanation, silanation/amidation, and the use of cyanuric chloride as a linking agent) and the merits of each are evaluated. The relationship between the observed properties of the attached arenes and the potential utility of the derivatized electrodes as anodes in photogalvanic cells is discussed.

## Introduction

Covalent modification of semiconductor electrodes used in photoelectrochemical cells has been studied recently as a

method for improving electrode stability,<sup>1</sup> for opening new electrocatalytic pathways,<sup>1,2</sup> and for attaching absorptive sensitizing dyes.<sup>3-6</sup> Our own interest in electron injection from